Search for the Higgs Boson in the Channel $H \rightarrow ZZ^{\star} \rightarrow 4\ell$ with the ATLAS Detector

Daniela Rebuzzi[1], *on behalf of the ATLAS Collaboration*

(1) Pavia University and INFN - Sezione di Pavia, Via A. Bassi, 6, 27100, Pavia, Italy

ATL-PHYS-PROC-2009-127
15 October 2009

Abstract

The search for the Standard Model Higgs boson is a major goal of the Large Hadron Collider (LHC). The Higgs boson mass is a free parameter in the Standard Model, however there is strong expectation motivated by precision electroweak data [1] and direct searches from LEP-2 [2] (Higgs boson ligther than 114.1 GeV/c^2 excluded) and Tevatron [3] (Higgs boson masses between 160 and 170 GeV/c^2 excluded at 95%CL) that a low mass Higgs boson ($m_H < 157$ GeV/c^2 at 95% CL, limit which becomes $m_H < 186$ GeV/c^2 when including the LEP-2 direct search limit - August 2009) should be discovered at LHC.

The decay channel $H \rightarrow ZZ^* \rightarrow 4\ell$ ($\ell = e, \mu$) provides a clean signature for the Higgs boson in the mass range between ~120 GeV/c^2 and $2M_Z$, above which the "gold-plated" channel, with two on mass-shell Z bosons in the final state, opens up.

The signal cross section is several orders of magnitude smaller than those for the backgrounds, therefore a thorough understanding of the multi-lepton processes is needed to obtain a high background rejection. Crucial for this channel is also a very good knowledge of the trigger and detector response for lepton identification and reconstruction.

The observability of the signal on top of the reducible $t\bar{t}$, $Zb\bar{b}$ and WZ and of the irreducible ZZ backgrounds with the ATLAS Detector [5] is discussed in the following, with particular emphasis on lepton reconstruction. The ATLAS discovery potential for the $H \rightarrow 4\ell$ channel, including the most realistic and up-to-date description of the detector performance, is presented.

1. $H \rightarrow ZZ^* \rightarrow 4\ell$ Channel

The SM Higgs production at LHC proceed essentially through two main processes, gluon-gluon fusion, dominant over all the whole mass range, and WW, ZZ fusion, which accounts for $\mathcal{O}(10\%)$ of the total cross section. The first process is know at NNLO with an uncertainty (coming from parton distribution functions and QCD scales) of around 10-20%. The vector-boson fusion process is known instead at NLO, with uncertainty smaller than 10%. The Higgs decay branching ratios, are currently also known up to NLO, with few percent of uncertainty. For the signal, PYTHIA event generator has been used (for both gluon and vector-boson fusion), rescaling its LO cross sections by the respective K-factors, to account for the higher order effects [4].

Table 1 reports the values of the $H \rightarrow ZZ^* \rightarrow 4\ell$ cross sections at LO and NLO, including the branching ratios into four leptons. Higgs boson masses between 120 and 600 GeV/c^2 have been evaluated and the correponding event samples have been processed thorugh the ATLAS full simulation and reconstruction chain.

For the backgrounds, various event generators have been adopted, and their cross sections rescaled to NLO [4]. Including the branching ratio into 4ℓ, they amount to 6.1 pb for $t\bar{t}$, 812.1 fb for $Zb\bar{b}$ and 34.8 $\cdot[K(M_{ZZ})+0.3]$ fb for ZZ, where $K(M_{ZZ})$ is a mass dependent K-factor and 0.3 accounts for the gluon initiated process, missing in the (PYTHIA) generator.

Table 1. $H \rightarrow ZZ^* \rightarrow 4\ell$ cross section at 14 TeV/c^2.

m_H [GeV/c^2]	$\sigma_{LO}\cdot$BR [fb]	$\sigma_{NLO}\cdot$BR [fb]
120	1.68	2.81
130	3.76	6.25
180	3.25	5.38
200	12.39	20.53
300	7.65	13.32
600	1.53	2.53

2. Lepton Trigger and Reconstruction

The impact of the three-level ATLAS trigger chain [5] on $H \rightarrow ZZ^* \rightarrow 4\ell$ events has been evaluated. Only events fulfilling a given trigger selection (electron and muon trigger slices) are kept for the following analysis steps. The trigger efficiency of electrons for a selection threshold of $E_T^{thres} = 22$ GeV/c^2 (including electron identification and isolation cuts), is shown in Figure 1 as a function of the true electron transverse energy. The acceptance of the muon trigger as a function of the generated p_T for the threshold $p_T^{thres} = 20$ GeV/c, is shown in Figure 2. Here, the efficiency above threshold is explained by the geometrical coverage of the ATLAS muon Level 1 trigger detectors.

Single and dilepton trigger are considered for this analysis [4]. In the following, single-lepton menu requiring 10 GeV/c muon or 15 GeV/c^2 (isolated) electron thresholds are chosen as trigger selection.

The lepton reconstruction efficiency is defined as the ratio of reconstructed to generated leptons originating from Z decays, within $|\eta| < 2.5$ and $p_T(E_T) > 5$ GeV/c^2. Quality flags classify reconstructed electrons and muons. For electrons, the containment in the middle sampling of the ATLAS ElectroMagnetic Calorimeter (EMC) and isolation requirements are satisfied by the so-called *LooseElectron* definition. The additional requirement of lateral shower shape containment and of track quality corresponds to the *MediumElectron* definition. In Figure 3, the electron reconstruction efficiency is shown as a function of $|\eta|$. *MediumElectron*+CALOISO refers to *MediumElectron* fulfilling the calorimetric (using all cells) isolation requirement.

Muon identification in ATLAS relies on the Muon Spectrometer (MS) information for standalone reconstruction, as well as on Inner Detector (ID) and Calorimeters for the so-called *Combined* reconstruction. Segments and tracks found in the MS are associated with the corresponding tracks in the ID (optionally requiring isolation at the Calorimeter and ID level), in order to identify muons at their production vertex with optimal parameter resolution. Figure 4 shows the muon reconstruction efficiency for *Combined* and all muons as a function of $|\eta|$.

Both lepton trigger and reconstruction efficiencies will be measured from data using the *Tag&Probe* method [4].

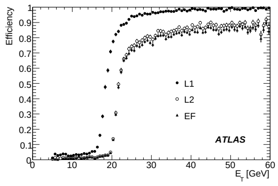

Fig. 1. Electron trigger efficiency for $E_T^{thres} = 22$ GeV/c^2.

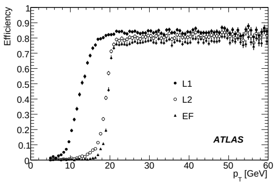

Fig. 2. Muon trigger efficiency for $p_T^{thres} = 20$ GeV/c.

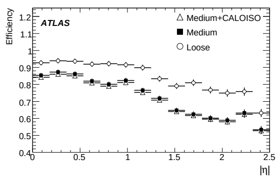

Fig. 3. Electron reconstruction efficiency.

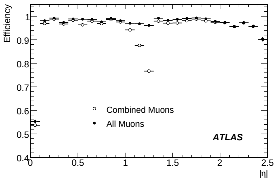

Fig. 4. Muon reconstruction efficiency.

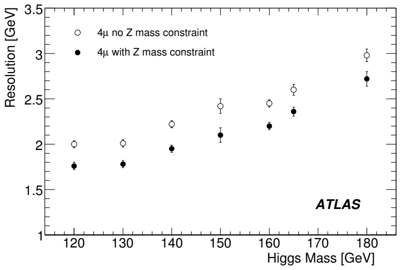

Fig. 5. $H \rightarrow 4\mu$ resolution as a function of the Higgs mass.

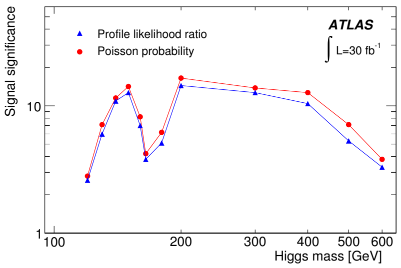

Fig. 6. Significance obtained using the Poisson statistics (circle, red curve) and from the profile likelihood ratio (triangles, blue curve), as a function of the Higgs boson mass.

3. Event Selection and Results

Events passing the trigger selection are required to further satisfy lepton preselection criteria. Electrons should be at least *LooseElectron* and have an $E_T > 5$ GeV/c^2 within $|\eta| < 2.5$. Muons are selected by requiring $p_T > 5$ GeV/c and $|\eta| < 2.5$. The final stage of event preselection requires at least four leptons with $p_T > 7$ GeV/c and $|\eta| < 2.5$, with at least two these leptons having $p_T > 20$ GeV/c.

The selection criteria then require events to have at least four leptons (e, μ) in pairs of same flavour and opposite charge. For Higgs boson masses below 200 GeV/c^2, electrons should at least be *MediumElectron*+CALOISO, while for higher Higgs boson masses, this cut can be relaxed to *LooseElectron*, due to the higher momentum of the decay electrons. When more than one quadruplet in the event is selected to be the Higgs boson candidate, the one with a dilepton mass closest to the nominal Z mass is chosen. Figure 5 shows the $H \rightarrow 4\mu$ resolution as a function of the Higgs boson mass. The resolution of (one or both) the dilepton mass(es) can be improved by 10% to 17% by applying a Z-mass constraint (i.e. a convolution between the nominal Z Breit-Wigner and a gaussian distribution centered at the measured Z value with σ equal to the experimental resolution). Similar results are obtained for the $4e$ and $2e2\mu$ channels.

Impact parameter and isolation (both in the EMC and in the ID) cuts have been also optimized against the *reducible* backgrounds, namely $Zb\bar{b}$ and $t\bar{t}$. Their combined applications result in a $\mathcal{O}(10^2)$ rejection for $Zb\bar{b}$ and $\mathcal{O}(10^2)$ rejection for $t\bar{t}$, keeping the signal efficiency above 80%.

Finally, a set of kinematic cuts is applied to the reconstructed Z invariant masses. These cuts have been optimized using the expected distributions for signal and backgrounds, and the expected dilepton resolution. The final significances are calculated separately for each of the three possible final states ($4e$, 4μ and $2e2\mu$) results are then combined together. Figure 6 shows the significance for an integrated luminosity of 30 fb^{-1}. Events are selected within a $m_H \pm 2\sigma_{m_H}$ mass window (where σ_{m_H} represents the experimental 4-lepton mass resolution). No systematic errors nor pile-up effects have been taken into account in the red curve, while the blue curve represents sthe signal significance calculated with a profile likelihood method, which takes into account most of the systematics uncertainties.

Uncertainties may come from theory or may have an experimental source. In the first case, they arise from parton distribution functions and QCD scales, which can affect the estimation of the cross section for signal and background, and thus the expected sensitivity up to a 20%. On the experimental side, signal significance extraction from real data is affected by systematics on the knowledge of lepton energy scale and resolution, lepton reconstruction efficiency, and reducible background knowledge from control samples (they have an overall impact on selection efficiency from 3.2% to 6.0% on the signal and from 3.1% to 5.4% on ZZ and $Zb\bar{b}$ backgrounds, the $t\bar{t}$ contribution is negligible). A 3% uncertainty on the luminosity should be also taken into account in the total systematic error calculation.

The effects of pile-up and cavern background in has been studied for an Higgs boson mass of 130 GeV/c^2. Its effect is to decrease the signal selection efficiency by about 10%, for all three decay channels, mostly due to a decrease in trigger and isolation cut efficiencies. Part of the loss can be recovered by reoptimization of the cuts.

References

[1] `http://lepewwg.web.cern.ch/LEPEWWG`.

[2] LEP Working Group for Higgs boson searches, CERN-EP-2003-011, Phys. Lett. B565:61-75,2003. e-Print: hep-ex/0306033.

[3] CDF and DZero Collaborations, *Combined CDF and DZero Upper Limits on Standard Model Higgs-Boson Production with up to 4.2 fb^{-1} of Data*, FERMILAB-PUB-09-060-E.

[4] ATLAS Collaborations, *Expected Performance of the ATLAS Experiment: Detector, Trigger and Physics*, CERN-OPEN-2008-020.

[5] ATLAS Collaborations, *The ATLAS Experiment at the CERN Large Hadron Collider*, J. Instrum. 3 (2008) S08003.